MODELING ULTRA FINE MIST TRANSPORT AND ITS IMPLICATIONS ON FIRE SUPPRESSION BEHAVIOR

K.C. Adiga
NanoMist Systems, LLC
151 Osigian Blvd, Suite 199, Warner Robins, GA 31088.
Voice: 478-953-2709 Email: kcadiga@nanomist.com

Ronald S. Sheinson, Frederick W. Williams and Scott Ayers[a,b]
Navy Technology Center for Safety and Survivability
Chemistry Division, Naval Research Laboratory
Washington DC 20375-5342

[a] Geo-Centers, Inc., 5813 Bayside Rd Building 307, Chesapeake Beach, MD 20732
[b] Current Address: Kidde Aerospace, 4200 Airport Blvd NW, Wilson, NC 27896

ABSTRACT

The last five years of research, development and testing of ultra fine water mist raised significant interest in its application for fire suppression and as an advanced inerting system. The objective of this work was to understand the transport behavior of ultra fine mist (UFM) under controlled discharge momentum which was intended to reduce the number of droplets coming into contact with surfaces and plating. This work was mainly focused on exploring the reasons for requiring dense gas model (DGM) approximation and solving convection-diffusion equations as opposed to the Lagrangian, Discrete Phase Model (DPM) generally applicable to a high momentum spray stream. The work showed that at high convective flow, DPM and DGM model predictions are close and transport time scales are not far off. However, at relatively weak flow conditions, the DPM model under-predicts the transport timescale and does not agree with experimental results. At this flow limit, diffusion transport contributes significantly and the DPM two-phase flow model cannot account for this. The lack of a strong convective field in the current ultra fine mist flow is mainly responsible for its ability to flow around objects without significant deposition. The understanding of the UFM transport behavior provides a robust tool for engineering and integrating the UFM technology into fire protection systems.

INTRODUCTION

More than half a decade of work on ultra fine water mist has shown that, under some selected process conditions, the mist transport and extinction behaviors are comparable or superior to Halon agents. The ultra fine water mist with droplet diameter below 10-micron closely resembles gaseous agents in transport behavior in cluttered spaces with a superior ability to diffuse around obstructions without significant loss of mist due to deposition [1-7]. A considerable amount of work has been reported on characterization, droplet behavior and mist fire suppression behavior under different laboratory conditions [8-12]. Although commercial water mist can be an efficient fire suppression agent, it has

not been effective when applied to volumes with significant obstructions. Further, as compared to ultra fine mist, it requires large quantities of water, which cause wetting and collateral damage to the protected area and infrastructure. In order to explore the benefits of UFM, further work is needed to address: 1) UFM transport issues, and 2) scaling of ultra fine water mist for high throughput real-scale scenarios. This paper will address the mist transport issues while ongoing, proprietary NanoMist® work is focusing on the possibility of a seamless scaling of mist production [13-14].

In order to reduce droplet impact events and thus reduce the coalescence and plating of water droplets "contacting" the obstructing surface, the discharge momentum was reduced to the extent possible by way of extremely fine droplets and low velocity. The droplet momentum for a 1-micron droplet is on the order of 5.23×10^{-16} kg.m.s^{-1} (u=1.0 m/s; m= 5.23×10^{-16} kg). Compare this with the momentum of 100-micron droplet, typical of regular water mist droplet, with a velocity of 10 m/s of 5.23×10^{-9} (a factor of 10^7). Thus, the low velocity combined with an extremely small droplet mass provides the desirable gas-like behavior for ultra fine mist, not contacting and impacting on surfaces causing significant mist loss as shown in prior work [1-7]. At this limiting flow condition, the convection becomes weak and is comparable to diffusion transport that helps mist droplets go around objects.

This work addresses the requirement of using a convection-diffusion approach to predict the transport behavior of extremely fine mist rather than the generally used Lagrangian DPM approach. This issue was reported in our work published recently in Fire Safety Journal [1]. That work did not address the reasons why the DPM model predicted short time scale (~ 5 seconds) while the tests showed significantly slow mist transport (5-8 minutes).

OBJECTIVE

The objective of this work was to understand the transport behavior of ultra fine mist under controlled momentum conditions and to evaluate the modeling methodologies for predicting the time dependent mist concentration within a flooding volume.

The specific objective was to determine the reasons for requiring a dense gas approximation and the solution for convection-diffusion transport modeling for ultra fine mist as opposed to the usually adopted Lagrangian droplet tracking approach used for high momentum droplet flows.

MODELING AND EXPERIMENTS

CFD Modeling

The Fluent CFD program was used to model flow, turbulence, energy and species transport [15]. The UFM transport and vaporization was modeled using the Discrete Phase Model in Fluent. The Lagrangian discrete phase uses the Euler-Lagrange approach. The fluid phase is treated as a continuum by solving the time-averaged Navier-Stokes equations, while the dispersed phase is solved by tracking a large number

of particles, bubbles, or droplets through the calculated flow field. The dispersed phase can exchange momentum, mass, and energy with the fluid phase. The particle or droplet trajectories are computed individually at specified intervals during the fluid phase calculation. This model is appropriate for simulating high momentum spray, but its application to a very weak flow is the topic of this study.

The trajectory of a discrete phase particle (or droplet or bubble) is obtained by integrating the force balance on the particle, which is written in a Lagrangian reference frame. This force balance equates the particle inertia with the forces acting on the particle, and can be written (for the x direction in Cartesian coordinates) as

$$\frac{du_p}{dt} = F_D(u - u_p) + \frac{g_x(\rho_p - \rho)}{\rho_p} + F_x \tag{1}$$

where F_x is an additional acceleration (force/unit particle mass) term, $F_D(u - u_p)$ is the drag force per unit particle mass and

$$F_D = \frac{18\mu}{\rho_p d_p^2} \frac{C_D \mathrm{Re}}{24} \tag{2}$$

Here, u is the fluid phase velocity, u_p is the particle velocity, μ is the molecular viscosity of the fluid, ρ is the fluid density, ρ_p is the density of the particle, and d_p is the particle diameter. Re is the relative Reynolds number, which is defined as

$$\mathrm{Re} \equiv \frac{\rho d_p |u_p - u|}{\mu} \tag{3}$$

The dispersion of particles due to turbulence in the fluid phase can be predicted using the stochastic tracking model or the particle cloud model. The stochastic tracking (random walk) model includes the effect of instantaneous turbulent velocity fluctuations on the particle trajectories through the use of stochastic methods

The CFD package, FLUENT, solves conservation equations for mass and momentum; additional equations for energy conservation, and species conservation equations are solved as well. Additional transport equations are also solved when the flow is turbulent.

The equation for conservation of mass, or the continuity equation, can be written as follows:

$$\frac{\partial \rho}{\partial t} + \nabla \cdot (\rho \vec{v}) = S_m \tag{4}$$

Equation (4) is the general form of the mass conservation equation and is valid for incompressible as well as compressible flows. The source $\mathbf{S_m}$ is the mass added to the continuous phase from the dispersed second phase (e.g., due to vaporization of liquid droplets) and any user-defined sources.

Conservation of momentum in an inertial (non-accelerating) reference frame is described

$$\frac{\partial}{\partial t}(\rho\vec{v}) + \nabla \cdot (\rho\vec{v}\vec{v}) = -\nabla p + \nabla \cdot (\bar{\bar{\tau}}) + \rho\vec{g} + \vec{F} \qquad (5)$$

where $\boldsymbol{p}$ is the static pressure, $\boldsymbol{\tau}$ is the stress tensor (described below), and ρg and $\boldsymbol{F}$ are the gravitational body force and external body forces respectively. These arise from interaction with the dispersed phase.

The stress tensor $\boldsymbol{\tau}$ is given by

$$\bar{\bar{\tau}} = \mu\left[(\nabla\vec{v} + \nabla\vec{v}^{\,\mathrm{T}}) - \frac{2}{3}\nabla \cdot \vec{v}I\right] \qquad (6)$$

Where, $\boldsymbol{\mu}$ is the molecular viscosity, $\boldsymbol{I}$ is the unit tensor, and the second term on the right hand side is the effect of volume dilation.

For an arbitrary scalar $\boldsymbol{\phi}$, Fluent CFD [15] solves the equation

$$\frac{\partial \rho\phi_k}{\partial t} + \frac{\partial}{\partial x_i}(\rho u_i \phi_k - \Gamma_k \frac{\partial \phi_k}{\partial x_i}) = S_{\phi_k} \quad k = 1, ..., N \qquad (7)$$

where $\boldsymbol{\Gamma_k}$ and $\boldsymbol{\phi_k}$ are the diffusion coefficient and source term supplied for each of the $\boldsymbol{N}$ scalar equations. Note that $\boldsymbol{\Gamma_k}$ is defined as a tensor in the case of anisotropic diffusivity. The diffusion term is thus:

$$\nabla \cdot (\boldsymbol{\Gamma_k} \cdot \phi_k)$$

The above conservation equation has both convective and diffusive flux. The scalar $\boldsymbol{\phi}$ will define for enthalpy $\boldsymbol{h}$, species $\boldsymbol{Y_i}$, and turbulence equations $\boldsymbol{k}$ and ϵ are for problems where heat transfer and species conservation are considered.

For turbulence modeling, the standard $\boldsymbol{k}$ - ϵ model is a semi-empirical model based on model transport equations for the turbulence kinetic energy ($\boldsymbol{k}$) and its dissipation rate (ϵ).

All individual terms, scalar equations and associated terms are defined in Fluent User Guide [15].

RESULTS AND DISCUSSION

As described earlier, the previous study on ultra fine mist total flooding fire tests showed that the DPM model transport time prediction was an order of magnitude shorter when compared to experiments as shown in Figure 1A and B. The DGM model gave closer agreement to measured water concentration [1]

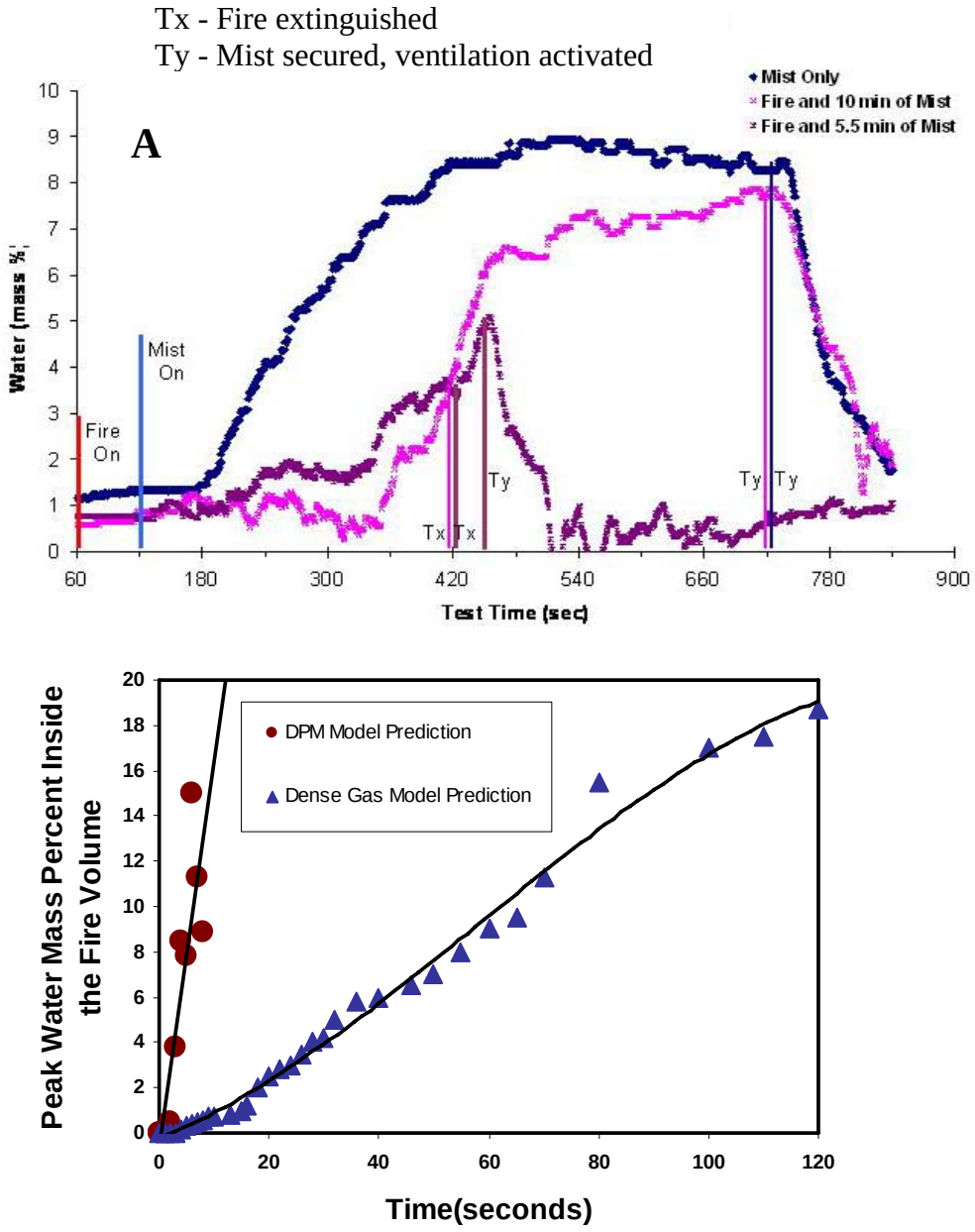

Figure 1: Comparison of A) measured water concentration history near the firebase and B) DPM and Dense Gas Model predictions in compartment fire tests. 1B computation times 0 – 120 sec correspond to 1A test times of 120 – 240 seconds.

This behavior of ultra fine mist at low momentum motivated further work in order to understand the reasons for the observed modeling discrepancies. The Understanding the discrepancy between the DPM model being valid for strong convective flow conditions and its inability to reproduce low momentum ultra fine mist behavior is the main objective of this work.

Figure 2 shows the geometry of the flow channel used for both DPM and dense gas model predictions. The flow geometry has a cross section 0.5 x 0.5 m and length 1.5 m. Predictions are taken at the centerline of the channel, x-z mid plane, and x-y plane-1 as show in Figure 2. The geometry had a slightly converging outlet in order to reduce the backflow into the calculation domain.

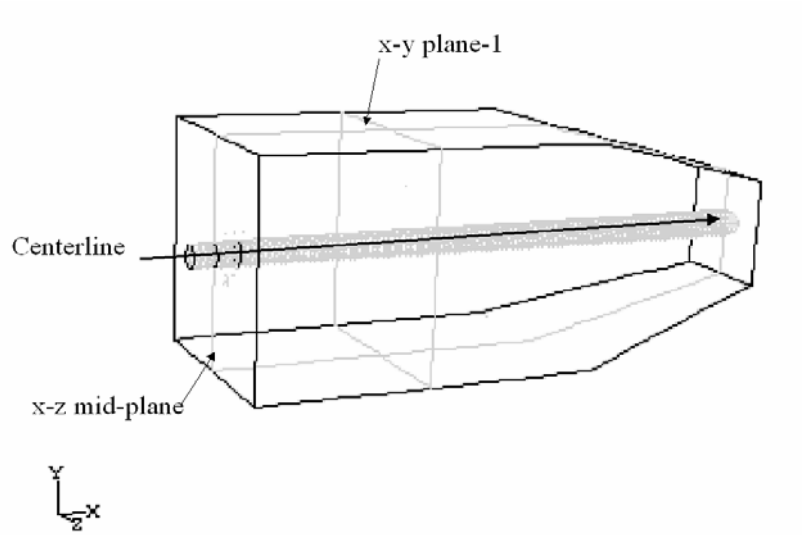

Figure 2: Geometry of flow channel used for simulating ultra fine mist flow

Comparison of Mist concentration profiles inside the channel:

A comparison of DPM and dense gas model (DGM) mist concentrations is shown in Figures 3A and B on the x-z middle plane (shown in Fig.2), at 2s after starting the mist. Droplets are monodispersed with 1-micron diameter. The contours predicted by DGM resembles dispersion of water mist in experiments; slowly spreading axially as well as radially. The mass fraction concentration gradient across the axial distance is very steep from the inlet at about 0.15 and at the outlet 0.01 showing a relatively slow transport. This behavior resembles ultra fine mist dispersion seen in experiments. However, the DPM model predicted an axially concentrated stream (without much radial dispersion) of mist with nearly uniform concentration, within 2 seconds. These contour plots show a relatively faster transport of water mist predicted by the DPM model as compared to the dense gas model. As indicated before, the DGM predictions are closer to prior experiments, which will be shown later.

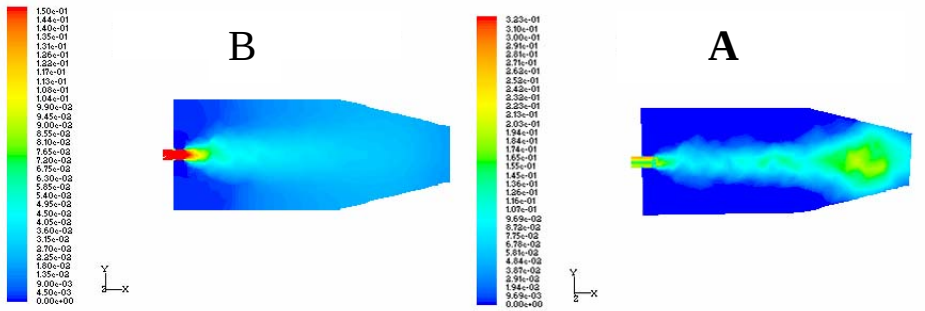

Figure 3: Predicted water concentration by: A) Dense Gas Model (DGM) and B) DPM at t=2 s using discharge velocity 5.0 m/s

The following section demonstrates detailed differences between DPM and DGM predictions, using simulations with varying mist discharge velocities from 1.0 m/s (a weak convective field close to free convection) to a strong convective field with a velocity of 25 m/s.

Dense Gas Model predictions:

Figure 4A and B show water concentrations predicted by the DGM model along the centerline of the channel at increasing time intervals. At a low velocity of 1.0 m/s, the centerline concentration builds up slowly to 180 seconds, as seen in Fig.4A. Even at 180s, the mist concentration at the end of the channel is significantly lower compared to the inlet concentration. However, in a strong convective field with a discharge velocity of 25 m/s, the mist is transported quickly downstream, as expected (Fig.4B). This behavior resembles the DPM transport prediction at low velocities. The rate of mist transport predicted by the DGM is shown by water mass fraction histories at different discharge velocities in Figure 5. The sharp increase in mist concentration at high velocity (u=25 m/s) shows the role of the convective field on the transport behavior. As the velocity increases, the mist concentration rises quickly, similar to the DPM model, shown in the next section.

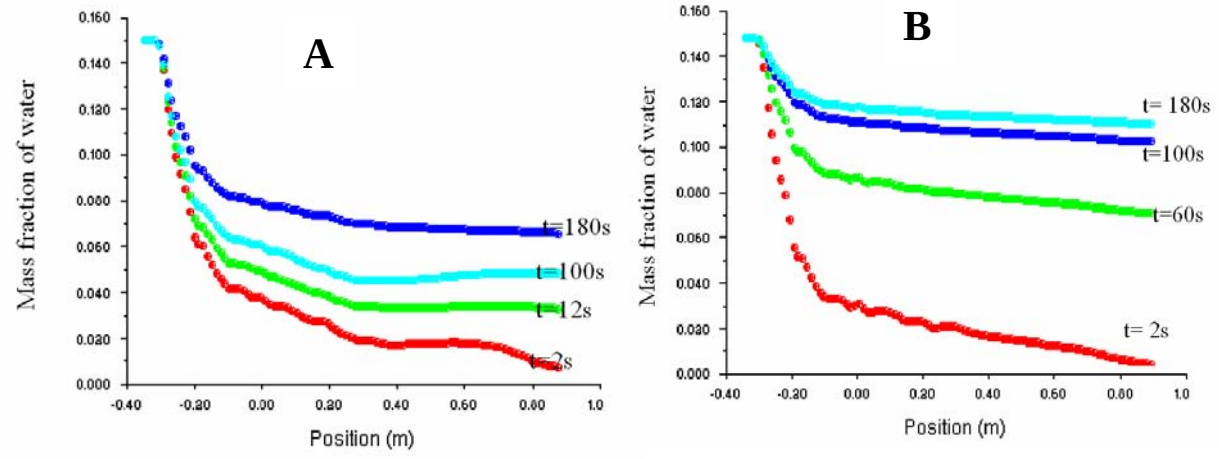

Figure 4: DGM centerline concentration of mist at various time steps for: A) a low discharge velocity of 1.0 m/s, and 2) a high discharge velocity of 25 m/s.

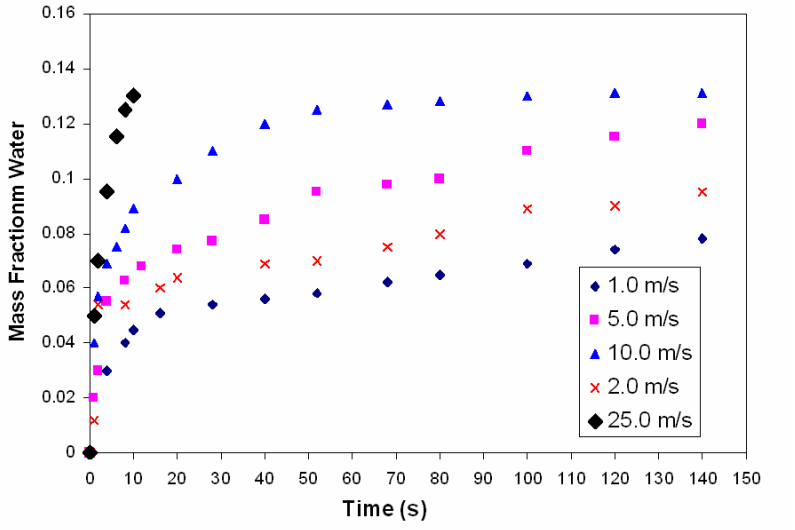

Figure 5: Time-dependent water mass fraction maximum at x-y plane-1 normal to flow -DGM Model

Discrete Phase Model (DPM) Prediction

DPM water concentration histories at a low discharge velocity of 1 m/s and a high velocity of 5 m/s are shown in Figures 6A and B respectively. The mist concentration spreads quickly in the axial direction even at 10-15 seconds as opposed to 150-180 seconds taken by the DGM model to reach similar concentrations. This is faster than DGM predictions by a factor of 10. The fluctuations in concentrations are due to stochastic tracking of droplets and are within the usual variations. The rate of buildup of concentration is clearly independent of final concentration at the plane unlike in diffusion dominated species transport. This is obvious from the fact that the rate did not decrease with time. This is inherent in the DPM because droplets are plunged into a continuum flow field with a time dependent stochastic tracking method of their position. Unlike in a diffusion dominated (weak convection) flow, the rate does not fall off as the concentration builds up at the target location.

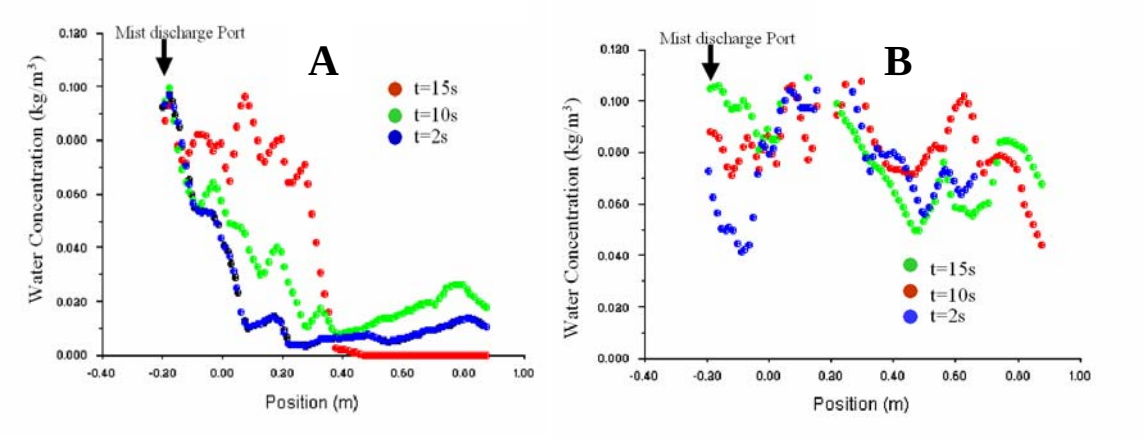

Figure 6: DPM centerline concentration of mist at various time steps for: A) a low discharge velocity of 1.0 m/s, and 2) a high discharge velocity of 5 m/s.

As shown in Figure 7, in the DPM modeling context, the mist concentration builds quickly, within 5-10 seconds, depending on the discharge velocity. This is similar to DGM predictions at 25 m/s where convection was strong (Fig.5, u=25 m/s). Since DPM predicted this fast build up of water concentration even at a relatively low flow field, it was necessary to adapt the use of the dense gas modeling approach.

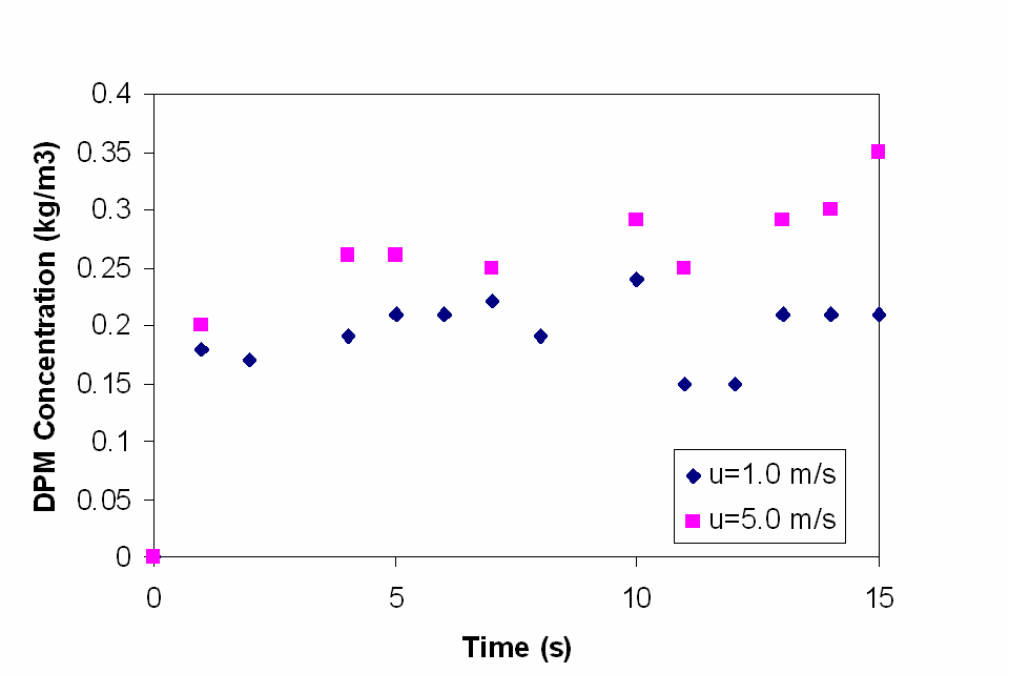

Figure 7: Time-dependent water mass fraction maximum at x-y plane-1 normal to flow -DGM Model

Low momentum gas like flow behavior in a obstructed channel

The dense gas model simulation of ultra fine mist in a flow channel with multiple staggered baffles is shown in Figure 8A. The flow is shown in terms of contours of mist (water). Predicted mist dispersion is similar to the usually observed ultra fine mist flow. Although not matching exactly in dimensions and baffle configuration, Figure 8B shows a photograph of an ultra fine mist flow in a flow channel with staggered baffles. The mist flows like a gaseous agent passing through sharp turns and reaching corners. The DGM prediction reproduces the overall flow behavior well within the obstructed flow channel.

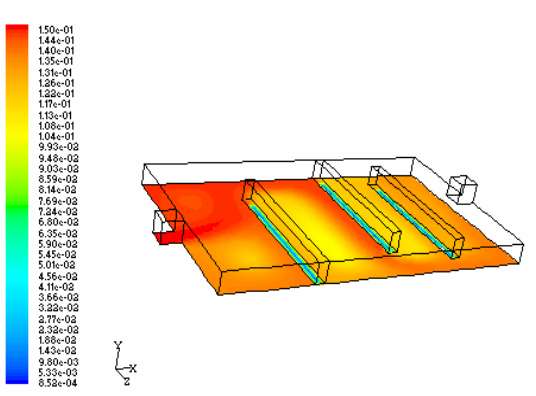

Figure 8A: Dense gas model mass fraction contours

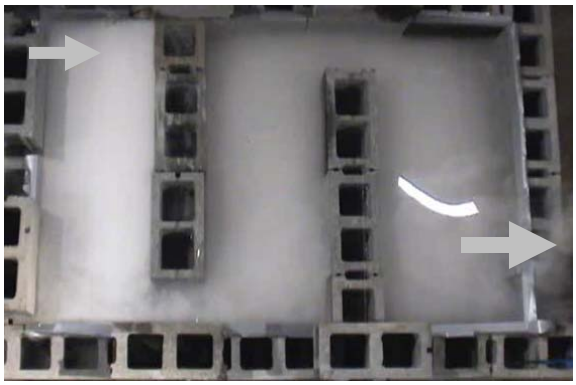

Figure 8B: Ultra fine mist flow experiment in a flow channel

CONCLUSIONS

At strong convective flow fields, the behavior of ultra fine mist transport can be reproduced using a dense gas model, DGM or DPM model. At these high velocity discharges, the transport rate is relatively fast and both model predictions are close to each other. They differ significantly, however, at very weak convective flows (1.0-2.0 m/s) where diffusion transport contributes significantly to the overall transport. Here, the mist dispersion behavior is slow and is similar to a dense gaseous species at low velocities. In these cases, the DPM predicts the droplets will be transported in the predominant flow direction without significant lateral dispersion, resulting in under-prediction of transport time. However, the dense gas model reproduces the lateral dispersion as well as the axial flow resembling a dense species convection-diffusion transport. The flow behavior of ultra fine mist at low momentum in an obstructed flow channel resembles such a dense gas flow. This behavior was the motivation for developing the current ultra fine mist technology with low momentum discharge and taking advantage of these traits in certain fire suppression application scenarios. The modeling options are crucial to produce a robust engineering design tool for new technology integration into the system.

ACKNOWLEDGEMENT

This work was partially funded as part of the Office of Naval Research (ONR) Future Naval Capabilities (FNC), Advanced Damage Countermeasures (ADC) program.

REFERENCES

1. Adiga, KC, Sheinson RS, Hatcher, Jr. RF, Williams FW and Ayers, S. A Computational and Experimental Study of Ultra Fine Water Mist as a Total Flooding Agent, Fire Safety J. l 42 (2007) 150–160
2. Adiga KC. Ultrafine water mist fire suppression technology, Fire Engineering, January 2005. p. 197-200.

3. Adiga KC, Adiga R and Hatcher Jr. RF. Self-entrainment of ultra fine water mist technology for new generation fire protection, Proceedings of Workshop on Fire Suppression Technologies, February 25-27, Mobile, Alabama (2003).
4. Adiga KC, Hatcher Jr. RF, Forssell EW, Scheffey JL, DiNenno PJ, Back III GG, Farley JP and Williams WW. False deck testing of Nanomist water mist systems, Proceedings Halon Options Technical Working Conference, Albuquerque, NM, 2005. http://www.bfrl.nist.gov/866/HOTWC/
5. Adiga KC and Williams FW. Ultra-fine water mist as a total flooding agent: A feasibility study, Proceedings Halon Options Technical Working Conference, Albuquerque, New Mexico, 2004. http://www.bfrl.nist.gov/866/HOTWC/
6. Adiga KC. A CFD study of the effects of inlet droplet variables on water mist fire suppression efficiency, Proceedings of the 36th Intersociety Energy Conversion Engineering Conference, 2001; Volume 1, Paper No. 2001-AT-77.
7. Sheinson RS, Ayers S, Williams FW, Adiga KC, Hatcher, Jr. RF. Feasibility evaluation study of very fine water mist as a total flooding fire suppression agent for flammable liquid fires, Proceedings Halon Options Technical Working Conference, Albuquerque, NM, 2004. http://www.bfrl.nist.gov/866/HOTWC/
8. Ndubizu CC, Ananth R, Williams FW. Effects of air-borne water mist on the local burning rate of a PMMA plate in boundary layer combustion, Proceedings Halon Options Technical Working Conference, Albuquerque, NM, 2004. http://www.bfrl.nist.gov/866/HOTWC/
9. Awtry AR, Fleming JW and Ebert V. Simultaneous diode-laser-based *in situ* measurement of liquid water content and oxygen mole fraction in dense water mist environments, Optics Letters 2006; 31, No 7, April 1, 2006, 900-902.
10. Ndubizu CC, Ananth R and Tatem PA. The effects of droplet size and injection orientation on water mist suppression of low and high boiling point liquid pool fires, Combust. Sci. and Tech. 2000; 157: 63-86.
11. Abbud-Madrid A, Lewis SJ, Watson JD, McKinnon JT and Delplanque JP. Study of water mist suppression of electrical fires for spacecraft applications: normal-gravity results. Proceedings Halon Options Technical Working Conference, Albuquerque, NM, 2005. http://www.bfrl.nist.gov/866/HOTWC/
12. Ndubizu CC, Ananth R, Williams FW. Suppression of small electrical cable fires with Fine water mist. Proceedings 4th Joint Meeting of the U.S. Sections of the Combustion Institute, 22 March 2005, Philadelphia, PA.
13. Adiga KC, Adiga R and Hatcher Jr. RF. Method and device for production, extraction and delivery of mist with ultra fine droplets, US Patent 6,883,724, April 26, 2005.
14. Adiga KC, Adiga R and Hatcher Jr. RF. Fire suppression using water mist with ultra fine size droplets, US Patent 7,090,028, April 15, 2006.
15. Fluent User's Guide Volumes 1-4, Fluent Incorporated, Central Resource Park, 10 Cavendish Court, Lebanon, NH 03766, Edn, 1998-2004